MOTION CONTROL OF HIGH-DIMENSIONAL MUSCULOSKELETAL SYSTEM WITH HIERARCHICAL MODEL-BASED PLANNING

Anonymous authors
Paper under double-blind review

ABSTRACT

Controlling high-dimensional nonlinear systems presents significant challenges in biological and robotic applications due to the large state and action spaces. While deep reinforcement learning has emerged as the leading approach, it suffers from being computationally-intensive and time-consuming, and are not scalable to wide varieties of tasks that each require significant manual tuning. This paper introduces Model Predictive Control with Morphology-aware Proportional Control (MPC^2), a novel hierarchical model-based algorithm that addresses these challenges. By integrating a sampling-based model predictive controller for target posture planning with a morphology-aware proportional controller for actuator coordination, our algorithm achieves stable movement control of a 700-actuator musculoskeletal model without training. We show that MPC^2 enables zero-shot high-dimensional motion control across diverse movement tasks, such as standing, walking on varying terrains, and sports motion imitation. It can be incorporated into optimal cost function design to automatically optimize the objective, reducing the reliance on traditional reward engineering methods. This work presents a major advancement in (near) real-time control for complex dynamical systems.

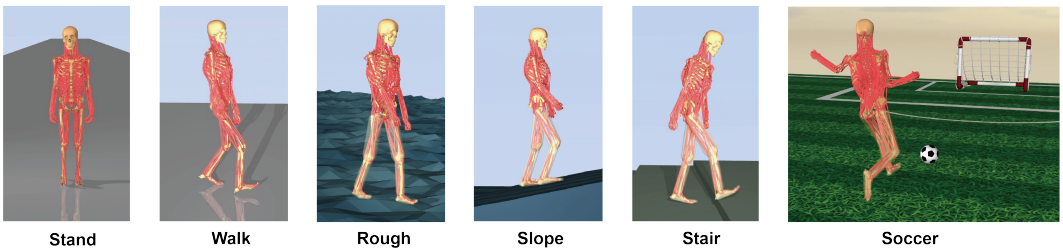

Figure 1: **Movement control of 700-dimensional human musculoskeletal system over a diverse set of motion control tasks.** The videos of the control performances and the code for experiment reproduction are in this anonymous link.

1 INTRODUCTION

High-dimensional nonlinear dynamical systems are prevalent in the real world, especially in biological musculoskeletal systems. The system complexity laid the foundation of flexible motion due to their over-actuated nature. The presence of additional actuation enhances the safety and robustness of the system, reducing the risk of performance degradation from actuator faults(Hsu et al., 1989). However, it also leads to large state and action spaces, posing significant challenges to achieving stable control performance. We take the human musculoskeletal system as a key example, where hundreds of muscles coordinate to facilitate various movements. Understanding and optimizing control in such systems is crucial for applications such as rehabilitation and human robot interaction (Kidziński et al., 2018; Vittorio et al., 2022).

To control such high-dimensional systems, various control methods have been proposed, with deep reinforcement learning (DRL) being the state of the art approach. However, RL approaches es-

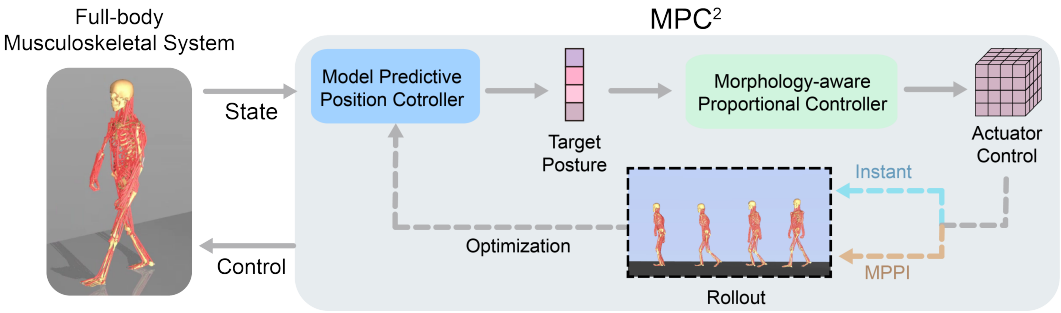

Figure 2: Workflow of Model Predictive Control with Morphology-aware Proportional Control (MPC^2). Solid arrows indicate control pipeline, and dashed arrows indicate planning procedure.

pecially struggle in high-dimensional state and action spaces, and typically necessitate the use of lower-dimensional representations. More importantly, the immense computational requirements of DRL impose a strict bottleneck on the iteration speed of reward engineering, meaning that researchers often require days (or longer) to discover effective control policies. Being able to generate effective control policies for high-dimensional nonlinear dynamical systems in *near real-time* is an open challenge.

Clinical studies on motor control of human movement revealed that predictive sampling is a crucial strategy in human movement control, such as maintaining balance during walking (Winter, 1991; Patla, 2003), where planning over a finite horizon determines the controls to be executed. Recent works have started to incorporate model predictive control (MPC) as the control backbone, offering faster behavior synthesis and more efficient reward design compared to DRL (Howell et al., 2022; Yu et al., 2023). However, effective planning in high-dimensional control spaces remains challenging, limiting the success of MPC primarily to low-dimensional systems. To the best of our knowledge, no training-free methods have achieved stable movement control of a whole-body musculoskeletal model across varying task conditions.

In this paper, we propose Model Predictive Control with Morphology-aware Proportional Control (MPC^2), a hierarchical model-based planning algorithm designed to address the challenges of high-dimensional musculoskeletal control. We introduce a sampling-based model predictive controller to plan the target posture of the agent, while a morphology-aware proportional controller serves as the low-level policy, adaptively coordinating the actuators to achieve the target joint positions. We demonstrate that our method can achieve stable control of a 700-actuator whole-body musculoskeletal model *without training*, enabling tasks such as standing, walking over varying terrain conditions, and sports motion imitation (Figure 1). Furthermore, we show that MPC^2's fast control generation facilitates efficient cost function optimization, improving task performance, especially for performing complex sequences of movement. The bottleneck in achieving *real-time* control with MPC^2 is the speed of the additional model forward dynamics computation, which can be solved by using more powerful computing devices or by controlling systems with reduced complexity.

Our contributions. (1) We propose MPC^2, the first MPC-based method capable of achieving near real-time stable control of high-dimensional musculoskeletal systems. (2) We demonstrate that our hierarchical model predictive control algorithm enables zero-shot high-dimensional full-body motion control across a wide range of motion tasks, many of which have not been achieved by state-of-the-art DRL-based methods. (3) We show that the much faster control generation latency of MPC^{2}facilitates automated cost function optimization via Bayesian optimization, demonstrating a pathway for reducing the human burden of reward engineering to near zero.

2 Related Work

2.1 High-dimensional musculoskeletal control

The control of musculoskeletal systems is challenging due to both high dimensionality and nonlinearity, with deep reinforcement learning (DRL) being the predominant choice in existing solutions

(Kidziński et al., 2018; Geiß et al., 2024). Hierarchical architectures are often employed to decompose control across different modules, where DRL provides high-level actions and a low-level policy generates muscle controls (Lee et al., 2019; Park et al., 2022; Feng et al., 2023). These approaches typically require large collections of motion data for imitation learning. Several works have also explored strategies to improve sample efficiency in over-actuated regime, including bio-inspired exploration (Schumacher et al., 2022), latent space exploration (Chiappa et al., 2023), model-based planning (Hansen et al., 2023), and multi-task learning (Caggiano et al., 2023). Recent studies have leveraged muscle synergies to reduce control dimensionality, enabling stable control across various musculoskeletal models (Berg et al., 2023; He et al., 2024). The aforementioned methods typically require many hours or even days of training to achieve effective control, and thus poses a significant bottleneck on the iteration speed of reward engineering.

2.2 Model predictive control for fast control generation

Compared to DRL, model predictive control allows for real-time control (Tassa et al., 2012), and thus has seen an increasing application of MPC in robotics, including tasks such as quadruped locomotion and dexterous manipulation (Kim et al., 2023). Recent works have also integrated MPC into the reward design process due to its training-free nature (Jain et al., 2021; Yu et al., 2023; Liang et al., 2024). However, MPC typically succeeds only in low-dimensional settings and often struggles when applied to high-dimensional problems. The most complex systems handled by existing MPC-based methods are typically torque-driven humanoids (Meser et al., 2024).

3 Preliminaries

3.1 Musculoskeletal system control

High-dimensional overactuated system. In this paper, we used MS-Human-700 as the target high-dimensional over-actuated system, which is a comprehensive whole-body musculoskeletal model with 90 rigid body segments, 206 joints, and 700 muscle-tendon units (Zuo et al., 2024). The dynamics of the system can be formulated as follows:

$$M(q)\ddot{q} + c(q, \dot{q}) = J_m^T f_m + J_c^T f_c + \tau_{ext}, \tag{1}$$

where q denotes generalized coordinates of joints, $M(q)$ denotes the mass distribution matrix, and $c(q, \dot{q})$ denotes Coriolis and the gravitational force, J_m and J_c denote Jacobian matrices that map forces to the generalized coordinates, f_c is the constraint force, f_m denotes actuator forces, and τ_{ext} denotes all external torque when interacting with environments.

MS-Human-700 is implemented in the MuJoCo physics simulator (Todorov et al., 2012), where actuators are modeled as first-order systems. The force generated by one actuator can be formulated as follows:

$$f_m = F_k \cdot a + F_p, \quad \frac{\partial a}{\partial t} = \frac{u - a}{(u - a)\tau_1 + \tau_2}, \tag{2}$$

where a is the actuator activation, F_k, F_p represents the gain and bias of the actuator force dynamics, u denotes the actuator control, τ_1 and τ_2 denote the time coefficients of the first-order actuator system.

Problem formulation. We treat the high-dimensional over-actuated control problem as a finite horizon Markov decision process with state $s \in \mathcal{S}$, control $u \in \mathcal{U}$, and dynamics f. For a given initial state of the model s_0 and a desired horizon T , we aim to find a control sequence $\boldsymbol{u}^\star_{0:T} = (u_0, ..., u_{T-1})$ that enable stable control, which can be achieved by minimizing the cumulative value of a task-specific cost function C_θ parameterized by θ:

$$\boldsymbol{u}^\star_{0:T} = \text{argmin}_{\boldsymbol{u}_{0:T}} \sum_{t=0}^{T-1} C_\theta(s_t, u_t), s_{t+1} = f(s_t, u_t) \tag{3}$$

In this paper, the definition of cost function C_θ is equivalent to the reward functions used in reinforcement learning (with negative value for maximization). For MS-Human-700, we consider the action space is $d_u = 700$-dimensional control of actuators (muscle-tendon units). The state space of the full-body model consist of joint positions and velocities, actuator activations and lengths, and task-related observations, leading to space dimensionality d_s over 1500.

3.2 SAMPLING-BASED MODEL PREDICTIVE CONTROL

Model predictive control is a general framework for model-based control, which optimizes a local control sequence using an approximated dynamics $\hat{f}$ within a short horizon $H \ll T$:

$$\hat{\boldsymbol{u}}^{\theta}_{t:t+H} = \text{argmin}_{\hat{\boldsymbol{u}}_{t:t+H}} \sum_{h=0}^{H-1} C_\theta(s_{t+h}, \hat{u}_{t+h}), s_{t+h+1} = \hat{f}(s_{t+h}, \hat{u}_{t+h}). \tag{4}$$

The optimized action sequence $\hat{\boldsymbol{u}}^{\theta}_{t:t+H} = (\hat{u}^{\theta}_t, \cdots, \hat{u}^{\theta}_{t+H-1})$ is a local approximation of optimal controls $\boldsymbol{u}^{\star}_{t:t+H}$. In real-world deployment where the action execution and planning are asynchronous, the planning horizon H should be chosen to balance accuracy and instantaneity.

Among various implementations of MPC frameworks, sampling-based MPC is a popular choice which samples local control sequences from a distribution of open-loop control sequences, $\hat{\boldsymbol{u}}_{t:t+H} \sim \boldsymbol{p}_\phi(\cdot)$, and update the sample distribution via parallel rollouts of the sampled action sequences. The objective of sampling-based MPC is to find a distribution parameter ϕ that minimize the cumulative cost function value of sampled action sequences. The distribution update process usually only depends on the rollout performance without direct operation on the states, which has been demonstrated success in the control of high degree-of-freedom systems, such as torque-driven humanoid models (Meser et al., 2024).

Model Predictive Path Integral (MPPI) control (Williams et al., 2016) is a commonly used sampling-based MPC method, which assumes the sampling distribution is a factorized Gaussian with $\phi = (\mu_t, \cdots, \mu_{t+H-1}, \sigma_t, \cdots, \sigma_{t+H-1})$:

$$\boldsymbol{p}_\phi(\hat{\boldsymbol{u}}_{t:t+H}) = \prod_{h=0}^{H-1} \mathcal{N}(\hat{u}_{t+h}; \mu_{t+h}, \sigma_{t+h}). \tag{5}$$

During the rollout process, N action sequences $\{\hat{\boldsymbol{u}}_{t:t+H}\}_{n=1}^{N}$ are sampled and executed via approximated transition $\hat{f}$. For each sampled sequence $\hat{\boldsymbol{u}}^{n}_{t:t+H}$, the cumulative cost function $\mathcal{C}^n_\theta = \sum_{h=0}^{H-1} C_\theta(s_{t+h}, \hat{u}^n_{t+h})$ is collected and used for distribution update:

$$\mu_{t+h} = \frac{\sum_{n=1}^{N} w_n \cdot \hat{u}^n_{t+h}}{\sum_{n=1}^{N} w_n}, \sigma_{t+h} = \sqrt{\frac{\sum_{n=1}^{N} w_n \cdot (\hat{u}^n_{t+h} - \mu_{t+h})^2}{\sum_{n=1}^{N} w_n}}, \quad 0 \le h \le H-1, \tag{6}$$

where $w_n = \mathbb{1}_{r(n) \le m} e^{-\frac{1}{\lambda}\mathcal{C}^n_\theta}$, $r(n)$ is the increasing-order rank of cumulative cost function value of rollout n, m is the number of elite rollouts, and λ is the temperature parameter.

3.3 OPTIMAL COST FUNCTION DESIGN

The finite-horizon optimization of MPC can result in a myopic policy, which may be suboptimal when evaluated in the long term. Recent studies demonstrate that the parameters of the cost function can be optimized to compensate for the issues induced by local optimization, which can be different from the true cost function measured in the full horizon T (Jain et al., 2021; Le & Malikopoulos, 2023). The objective of optimal cost function design is to find parameters θ^* that minimizes the cumulative value of true cost function C_θ over the horizon T:

$$\theta^* = \text{argmin}_{\theta'} \sum_{t=0}^{T-1} C_\theta(s_t, \hat{u}^{\theta'}_t), s_{t+1} = f(s_t, \hat{u}^{\theta'}_t), \tag{7}$$

where $(\hat{u}^{\theta'}_0, \cdots, \hat{u}^{\theta'}_H - 1)$ is the control sequence of MPC optimized under cost function parameterized by θ'. As only zero-order cost function value can be accessed, e.q. 7 can be considered as a black-box optimization problem, which can be addressed by Bayesian optimization (Frazier, 2018) or evolutionary algorithms (Hansen, 2006)

Algorithm 1: Model Predictive Control with Morphology-aware Proportional Control (MPC^2)

Input: Model dynamics f, rollout horizon H, total rollout number N, instant rollout number $\bar{N}$, iteration number r, distribution parameter μ, σ, current state s_t

for $i = 1, \cdots, r$ **do**
- $z^1, ..., z^{\bar{N}} \sim \mathcal{N}(M_{\text{pos}}(s_t), \sigma)$ `// Instant rollout`
- $z^{\bar{N}+1}, ..., z^N \sim \mathcal{N}(\mu, \sigma)$ `// MPPI rollout`
- $\mathcal{C}_\theta^1, \cdots, \mathcal{C}_\theta^N \leftarrow \mathcal{R}_{\text{MP}}(z^1, H), \cdots, \mathcal{R}_{\text{MP}}(z^N, H)$
- Update μ, σ using e.q. (6)

end

$z^* \leftarrow \mu, \quad \hat{u}_t^\theta \leftarrow \pi_{\text{MP}}(s_t, z^*)$

return $\hat{u}_t^\theta, z_*, \mu, \sigma$

4 Model Predictive Control with Morphology-Aware Proportional Control (MPC^2)

Existing approaches for controlling high-dimensional musculoskeletal systems often incorporate deep reinforcement learning as a central component, where a state-feedback policy, $\pi(u|s)$, is learned from interactions with the model dynamics. While substantial efforts have been made to reduce the dimensionality of the action space, the large state space continues to present significant challenges for policy training. In this paper, we opt to use model predictive control instead of deep reinforcement learning for the following reasons: (1) The overall control is conducted in simulation, where the exact dynamics is accessible, that is $\hat{f} = f$; and (2) the use of sampling-based MPC circumvents the challenge of decision-making in high-dimensional state spaces. (3) MPC offers much faster control generation, enabling more reward design iterations than DRL. We consider these features significant advantage of sampling-based MPC over DRL-based methods.

However, directly deploying MPC on musculoskeletal systems is challenging. High-dimensional control space poses large obstacles for generating control sequences for movement. In this section, we demonstrate that applying MPC to such problems is indeed possible. In biological systems such as vertebrates, hierarchical control strategies are widely observed, where sensory information is processed by a high-level controller for planning, while motor commands are generated by a low-level controller based on proprioception (Merel et al., 2019). This enables diverse motion control without specific training. To this end, we introduce MPC^2, a hierarchical MPC method that facilitates stable control of high-dimensional musculoskeletal systems, as shown in Figure 2 and Algorithm 1. MPC^2 has two major components: (1) a model predictive position controller as the high-level planner which optimize for the target posture z^* given current state s_t; and (2) a morphology-aware proportional controller $\pi_{\text{MP}}(u|s, z)$ as the low-level policy which computes actuator controls to achieve the target posture from given state.

4.1 Model predictive position control

We employ MPC over the planning of major joint coordinates z that determine the system posture. For MS-Human-700, the dimension of z is $d_z = 37$. Compared to torque, we choose lower-order joint position as the MPC objective to reduce the control frequency. Therefore, only one target posture z is required to optimize during one rollout, where our morphology-aware proportional controller adapts control signals based on the instant states:

$$\mathcal{C}_\theta = \mathcal{R}_{\text{MP}}(z, H) = \sum_{h=0}^{H-1} C(s_{t+h}, u_{t+h}), u_{t+h} = \pi_{\text{MP}}(s_{t+h}, z). \tag{8}$$

Compared to planning over original action space, MPC^2 significantly reduce the number planning parameters from $H \cdot d_u$ to d_z, enabling optimizing controls via sampling. While the original Model Predictive Path Integral (MPPI) can be directly employed as a high-level planner for target positions, we find that it lacks the ability to respond quickly to rapidly changing states, such as when the agent is falling. This issue cannot be easily mitigated by simply increasing the number of rollouts, as only a

limited number (at most a few dozen) can be executed in parallel when controlling high-dimensional systems, due to both computational budget constraints and the need for real-time responsiveness.

To equip MPC with rapid response capabilities for changing states, we leverage the feature of position control and propose the use of *instant rollouts* during planning (line 2 in Algorithm 1). Rather than sampling based on the policy from the previous planning iteration, instant rollouts sample target postures based on the model's current posture, which can be extracted from the current state using a posture mask: $z_t = M_{\text{pos}}(s_t)$. When the current state significantly deviates from the previous planning state, this approach provides a better initial point compared to the original MPPI samples, increasing the likelihood of sampling more effective controls to re-stabilize the agent. We will demonstrate the necessity of instant rollouts for position control in the experimental section.

4.2 Morphology-aware proportional control

Here we introduce the morphology-aware proportional controller $\pi_{\text{MP}}(u|s, z)$, a key component for reducing the control dimensionality, which coordinates actuator controls to adapt to the target posture. Given the target joint coordinate z^*, the target actuator length l^* can be computed with model forward dynamics. We define proportional controllers for each actuator, which determine the actuator force required to achieve the target actuator length given current actuator length l:

$$f_m^* = \min(0, k \cdot (l^* - l)), \tag{9}$$

where k is the proportional gain parameter. Utilizing the first-order actuator dynamics in 2, we are able to derive the control signal u^* to achieve target actuator force f_m^* given current actuator activation a:

$$u^* = a + \frac{\tau_2(a^* - a)}{\Delta t - \tau_1(a^* - a)}, \tag{10}$$

where $a^* = (f_m^* - F_p)/F_k$ is the target actuator activation, and Δt is the duration of each time step. The proportion gain vector $K = (k_1, \cdots, k_{d_u})$ controls the scaling of target forces, which is critical for the control performance. Improper gain settings can result in excessive collisions (if too large), insufficient force generation (if too small), which should be individually set for each of the 700 actuators.

From system dynamics in e.q. 1, the conversion from actuator forces to joint torque is computed using the Jacobian matrices of the model, J_m, which can represent the influence of actuators on joint movements. Based on this observation, we propose to set proportional gains according to the system morphology. Instead of manually setting these gains, we set them based on the Jacobian matrices of current state and the target posture:

$$K = \bar{k} \cdot \sum_{i \in \mathcal{I}_z} |\text{col}_i(J_m) \cdot [z_i^* - M_{\text{pos}}(s_t)_i]|, \tag{11}$$

where $\bar{k}$ is the only scaling parameter, $\mathcal{I}_z$ is the indices of major joints z over all joints, $|\cdot|$ is the absolute value operator, and $\text{col}_{(\cdot)}(J_m)$ is the column operator of J_m. The Jacobian values vary according to different system posture, allowing for adaptive and efficient control of different motion.

Note that MPC^2 achieves high-dimensional musculoskeletal control through online planning using model dynamics, allowing for the control of complex behaviors without the need for a training procedure. This zero-shot motion control also enables rapid evaluation of cost function designs, facilitating efficient optimization of the cost function.

5 Experiments

In this section, we aim to comprehensively evaluate MPC^2, and seek to answer the following questions: **(1)** Can MPC^2 achieve robust and performant control over a wide variety of motion tasks? **(2)** Can we leverage the fast generation speed of MPC^{2}to serve as the inner loop in a cost function optimization problem? **(3)** How do the individual components of MPC^2 contribute to its overall effectiveness?

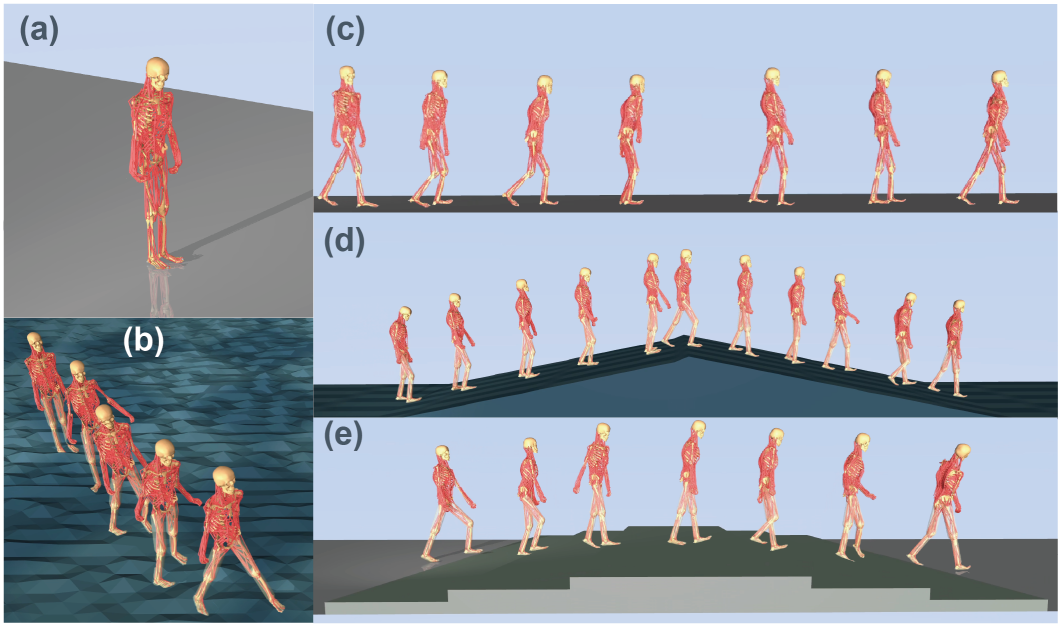

Figure 3: Control sequences of MPC^2 in (a) Stand, (b) Rough, (c) Walk, (d) Slope and (e) Stair tasks. The simulation speed of Stair task is set to 10% due to slower contact computation.

Tasks: We design the following control tasks, which consists of a wide range of human full-body motion (with individual cost function terms listed in Appendix C.):

Stand. This task requires standing still and keep balance for 10 seconds.
Walk. This task requires walking forward over a flat floor for 10 meters.
Rough. This task requires walking forward over a rough terrain for 10 meters.
Slope. This task requires walking up and down slopes.
Stair. This task requires walking up and down stairs.
Soccer. This task requires imitating a reference trajectory to kick the ball.

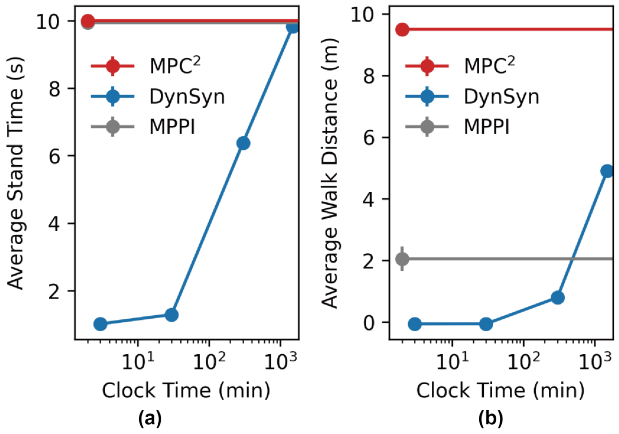

Figure 4: Control performance versus clock time (training time + deployment time). Results show the mean performance with one standard error, averaged over 50 independent trials.

Implementation details. We implement MPC^2 using the Mujoco MPC (MJPC) platform (Howell et al., 2022), a framework designed for real-time model predictive control. The MJPC platform supports asynchronous simulation between the main thread and planning, which we find to be more practical than freezing the main thread during planning. In all experiments, we set the iteration number r of MPC^2 to 1 for rapid response to the changing states in the main thread, and sample 64 rollouts (containing $\bar{N} = 10$ instant rollouts) across a 0.3s horizon during each round of planning. Unless otherwise noted, the simulation in main thread are run with 20% of the real-time speed (following Howell et al. (2022)), where control sequences to complete the task can be generated within 2 minutes. The experiments of MPC^2 were conducted on a server equipped with an AMD EPYC 7773X processor, an NVIDIA GeForce RTX 4090 GPU, and 512 GB of memory.

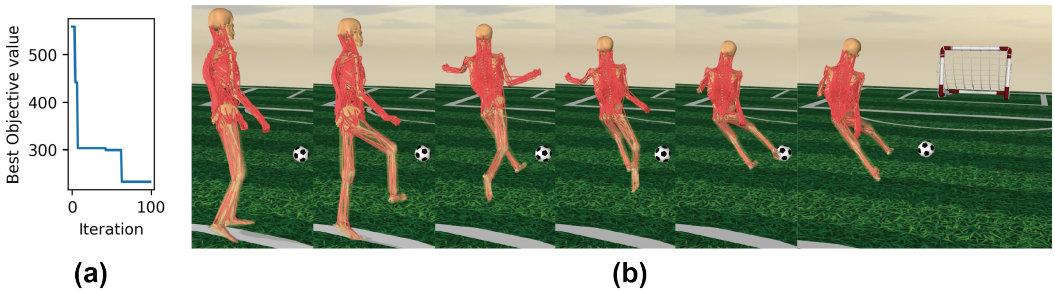

Figure 5: Motion control of Soccer task. (a) Cost function optimization performance. (b) Control sequences of MPC^2. The simulation speed is set to 1% for more frequent planning for rapidly changing motion, where the entire control sequence is learned within 4 minutes.

5.1 Full-body movement control

Motion control over different terrain. We show control sequences of the Stand, Walk, Rough, Slope, and Stair tasks using MPC^2 in Figure 3. While no previous control methods have demonstrated success in whole-body musculoskeletal systems for these tasks, MPC^2 exhibits consistent and stable control performance across various tasks, enabling navigation over different terrain conditions.

Comparison to RL. In the Stand and Walk-Flat tasks, we compared the control performance of MPC^2 with the current state-of-the-art DRL-based algorithms, DynSyn (He et al., 2024), which identify and utilize muscle synergies to reduce control dimensionality, and demonstrates stable walking control over whole-body musculoskeletal model. We also included the original MPPI (Williams et al., 2016) as a baseline to perform an ablation of our hierarchical pipeline. Figure 4 shows the total time required for control sequence generation. We observe that DynSyn requires at least one day to achieve effective control in both tasks. While MPPI is capable of maintaining balance in the Stand task, it struggles to generate control sequences for forward movement in the high-dimensional action space. MPC^2 enables stable standing and walking control within 2 minutes, demonstrating a significant time efficiency advantage over DynSyn for deployment.

5.2 Sports motion control with optimal cost function design

The fast control generation speed of MPC^2 enables rapid evaluation and iteration of cost function design. In settings where the true objective can be simply described, we can leverage black-box optimization algorithms to discover MPC cost functions that best optimize the true cost function, resulting in *automatic behavior synthesis*. If possible, this functionality is especially crucial in massively multi-task settings, where many complex behaviors must be generated.

We consider this problem in the setting of sports, which often require diverse and complex movements. As a case study, we investigate whether MPC^2 combined with a black-box optimizer can automatically learn to kick a soccer ball. We specifically use a Gaussian-process-based Bayesian optimization algorithm to optimize the weights of the position error terms for different body parts (Jones et al., 1998; Rasmussen, 2003; Ament et al., 2023). The optimization objective is the quadratic position error of each body part, with results shown in Figure 5(a). We observe that the cost objective effectively improves compared to the initial settings. Thanks to MPC^2's training-free control generation, our 100 cost design iterations take only around 5 hours, whereas DRL-based methods cannot even complete a single reward evaluation (i.e. a single trained policy) in that time frame. MPC^2 successfully imitates the reference trajectory and enables sports motion control, generating sufficient speed and force to kick the ball (Figure 5(b)).

5.3 Algorithm analysis

To understand superior control performance behind MPC^2 , we investigate both model predictive position controller and morphology-aware proposition controller. The analysis results is shown in Figure 6.

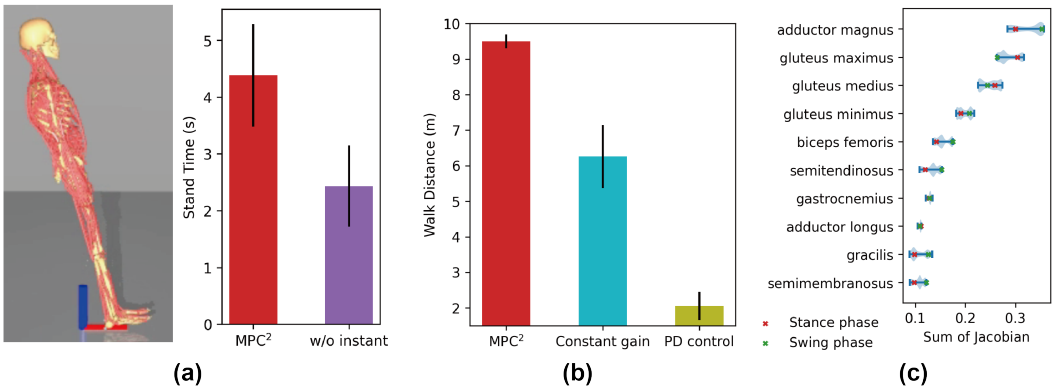

Figure 6: Analysis of MPC^2. Results show the mean performances with one standard error over 20 trials. (a) Control performance of lean backward standing, with initial position shown on the left. Blue axis indicates the vertical direction. (b) Control performance of the Walk task. (c) The distribution of absolute Jacobian summations of a walking trajectory.

Instant rollout for rapid planning. We modified the standing task to evaluate the effectiveness of the instant rollout component in high-level posture planning. As shown in Figure 6(a), instead of starting from an upright position, we set the initial posture of the model to lean significantly backward, requiring a rapid response to recover balance. Our results show that MPC^2 significantly outperforms its variant without the instant rollout, demonstrating that the instant rollout enables a timely response in unstable states.

Morphology-aware gain design. We compare MPC^2 with two variants over the low-level actuator controller side: (1) a proportional controller with constant gain settings for all actuators, which has a similar average actuator force as MPC^2, and (2) proportional-derivative (PD) control, setting the derivative gains based on the proportional gains. Figure 6(b) shows that MPC^2 significantly outperforms both the constant gain and PD control variants. In Figure 6(c), we observe that the system's Jacobian effectively identifies the major muscles involved during walking and adapts to different phases of motion. Our morphology-aware gain design automatically prioritizes the major actuators for more efficient control, demonstrating its fidelity in biomechanics.

6 Conclusion

In this paper, we propose MPC^2, a hierarchical model predictive control method designed to enable near real-time motion control of high-dimensional musculoskeletal systems without the need for training. The algorithm employs a high-level model predictive position controller for posture planning and utilizes a morphology-aware proportional controller to coordinate actuators in achieving the target posture. Using a whole-body model with 700 actuators, we demonstrate the stable control performance of MPC^2 across a wide range of movement tasks, as well as its fast controller generation for efficient cost function optimization. Ablation studies over the algorithm components further verify the principled design and biomechanical fidelity of MPC^2.

References

Sebastian Ament, Samuel Daulton, David Eriksson, Maximilian Balandat, and Eytan Bakshy. Unexpected improvements to expected improvement for bayesian optimization. *Advances in Neural Information Processing Systems*, 36:20577–20612, 2023.

Cameron Berg, Vittorio Caggiano, and Vikash Kumar. Sar: Generalization of physiological agility and dexterity via synergistic action representation. *arXiv preprint arXiv:2307.03716*, 2023.

Vittorio Caggiano, Sudeep Dasari, and Vikash Kumar. Myodex: a generalizable prior for dexterous manipulation. In *International Conference on Machine Learning*, pp. 3327–3346. PMLR, 2023.

Alberto Silvio Chiappa, Alessandro Marin Vargas, Ann Huang, and Alexander Mathis. Latent exploration for reinforcement learning. *Advances in Neural Information Processing Systems*, 36, 2023.

Yusen Feng, Xiyan Xu, and Libin Liu. Musclevae: Model-based controllers of muscle-actuated characters, 2023. URL https://arxiv.org/abs/2312.07340.

Peter I Frazier. A tutorial on bayesian optimization. *arXiv preprint arXiv:1807.02811*, 2018.

Henri-Jacques Geiß, Firas Al-Hafez, Andre Seyfarth, Jan Peters, and Davide Tateo. Exciting action: Investigating efficient exploration for learning musculoskeletal humanoid locomotion. *arXiv preprint arXiv:2407.11658*, 2024.

Nicklas Hansen, Hao Su, and Xiaolong Wang. Td-mpc2: Scalable, robust world models for continuous control. *arXiv preprint arXiv:2310.16828*, 2023.

Nikolaus Hansen. The cma evolution strategy: a comparing review. *Towards a new evolutionary computation: Advances in the estimation of distribution algorithms*, pp. 75–102, 2006.

Kaibo He, Chenhui Zuo, Chengtian Ma, and Yanan Sui. Dynsyn: Dynamical synergistic representation for efficient learning and control in overactuated embodied systems, 2024. URL https://arxiv.org/abs/2407.11472.

Taylor Howell, Nimrod Gileadi, Saran Tunyasuvunakool, Kevin Zakka, Tom Erez, and Yuval Tassa. Predictive sampling: Real-time behaviour synthesis with mujoco, 2022. URL https://arxiv.org/abs/2212.00541.

Ping Hsu, John Mauser, and Shankar Sastry. Dynamic control of redundant manipulators. *Journal of Robotic Systems*, 6(2):133–148, 1989.

Avik Jain, Lawrence Chan, Daniel S Brown, and Anca D Dragan. Optimal cost design for model predictive control. In *Learning for Dynamics and Control*, pp. 1205–1217. PMLR, 2021.

Donald R Jones, Matthias Schonlau, and William J Welch. Efficient global optimization of expensive black-box functions. *Journal of Global optimization*, 13:455–492, 1998.

Łukasz Kidziński, Sharada P Mohanty, Carmichael F Ong, Jennifer L Hicks, Sean F Carroll, Sergey Levine, Marcel Salathé, and Scott L Delp. Learning to run challenge: Synthesizing physiologically accurate motion using deep reinforcement learning. In *The NIPS'17 Competition: Building Intelligent Systems*, pp. 101–120. Springer, 2018.

Gijeong Kim, Dongyun Kang, Joon-Ha Kim, Seungwoo Hong, and Hae-Won Park. Contact-implicit mpc: Controlling diverse quadruped motions without pre-planned contact modes or trajectories. *arXiv preprint arXiv:2312.08961*, 2023.

Viet-Anh Le and Andreas A Malikopoulos. Optimal weight adaptation of model predictive control for connected and automated vehicles in mixed traffic with bayesian optimization. In *2023 American Control Conference (ACC)*, pp. 1183–1188. IEEE, 2023.

Seunghwan Lee, Moonseok Park, Kyoungmin Lee, and Jehee Lee. Scalable muscle-actuated human simulation and control. *ACM Transactions On Graphics (TOG)*, 38(4):1–13, 2019.

Jacky Liang, Fei Xia, Wenhao Yu, Andy Zeng, Montserrat Gonzalez Arenas, Maria Attarian, Maria Bauza, Matthew Bennice, Alex Bewley, Adil Dostmohamed, et al. Learning to learn faster from human feedback with language model predictive control. *arXiv preprint arXiv:2402.11450*, 2024.

Josh Merel, Matthew Botvinick, and Greg Wayne. Hierarchical motor control in mammals and machines. *Nature communications*, 10(1):1–12, 2019.

Moritz Meser, Aditya Bhatt, Boris Belousov, and Jan Peters. Mujoco mpc for humanoid control: Evaluation on humanoidbench. *arXiv preprint arXiv:2408.00342*, 2024.

Matthew Millard, Thomas Uchida, Ajay Seth, and Scott L Delp. Flexing computational muscle: modeling and simulation of musculotendon dynamics. *Journal of biomechanical engineering*, 135(2):021005, 2013.

Jungnam Park, Sehee Min, Phil Sik Chang, Jaedong Lee, Moon Seok Park, and Jehee Lee. Generative gaitnet. In *ACM SIGGRAPH 2022 Conference Proceedings*, pp. 1–9, 2022.

Aftab E Patla. Strategies for dynamic stability during adaptive human locomotion. *IEEE Engineering in Medicine and Biology Magazine*, 22(2):48–52, 2003.

Carl Edward Rasmussen. Gaussian processes in machine learning. In *Summer school on machine learning*, pp. 63–71. Springer, 2003.

Pierre Schumacher, Daniel Häufle, Dieter Büchler, Syn Schmitt, and Georg Martius. Dep-rl: Embodied exploration for reinforcement learning in overactuated and musculoskeletal systems, 2022. URL https://arxiv.org/abs/2206.00484.

Yuval Tassa, Tom Erez, and Emanuel Todorov. Synthesis and stabilization of complex behaviors through online trajectory optimization. In *2012 IEEE/RSJ International Conference on Intelligent Robots and Systems*, pp. 4906–4913. IEEE, 2012.

Emanuel Todorov, Tom Erez, and Yuval Tassa. Mujoco: A physics engine for model-based control. In *2012 IEEE/RSJ International Conference on Intelligent Robots and Systems*, pp. 5026–5033, 2012. doi: 10.1109/IROS.2012.6386109.

Caggiano Vittorio, Wang Huawei, Durandau Guillaume, Sartori Massimo, and Kumar Vikash. Myosuite – a contact-rich simulation suite for musculoskeletal motor control. https://github.com/myohub/myosuite, 2022. URL https://arxiv.org/abs/2205.13600.

Grady Williams, Paul Drews, Brian Goldfain, James M. Rehg, and Evangelos A. Theodorou. Aggressive driving with model predictive path integral control. In *2016 IEEE International Conference on Robotics and Automation (ICRA)*, pp. 1433–1440, 2016. doi: 10.1109/ICRA.2016.7487277.

David A Winter. *Biomechanics and motor control of human gait: normal, elderly and pathological*. 1991.

Wenhao Yu, Nimrod Gileadi, Chuyuan Fu, Sean Kirmani, Kuang-Huei Lee, Montse Gonzalez Arenas, Hao-Tien Lewis Chiang, Tom Erez, Leonard Hasenclever, Jan Humplik, et al. Language to rewards for robotic skill synthesis. *arXiv preprint arXiv:2306.08647*, 2023.

Chenhui Zuo, Kaibo He, Jing Shao, and Yanan Sui. Self model for embodied intelligence: Modeling full-body human musculoskeletal system and locomotion control with hierarchical low-dimensional representation. In *2024 IEEE International Conference on Robotics and Automation (ICRA)*, pp. 13062–13069, 2024.

A NEURO-MUSCLE DYNAMICS

We use the muscle-tendon units in MuJoCo as our actuator. The input control signal of muscle-tendon units is the neural excitation, denoted as u. The muscle activation, denoted as act, is calculated by a first-order nonlinear filter as follows:

$$\frac{\partial \text{act}}{\partial t} = \frac{u - \text{act}}{\tau(u, \text{act})}, \tau(u, \text{act}) = \begin{cases} \tau_{\text{act}} \left(0.5 + 1.5 \cdot \text{act}\right) & u > \text{act}, \\ \tau_{\text{deact}} / \left(0.5 + 1.5 \cdot \text{act}\right) & u \leq \text{act} \end{cases},$$

where τ_{act} and τ_{deact} represent the time constants for activation and deactivation latency, with default values of 10 ms and 40 ms. where $\tau(u, a)$ is the the effective time constant (Millard et al., 2013), which have been smoothed using sigmoid function in e.q. 2, as derived in the tutorial of MyoSuite[1].

The force produced by a single muscle-tendon unit is given by:

$$f_m(a) = f_{\text{max}} \cdot \left[F_l(l) \cdot F_v(v) \cdot a + F_p(l)\right],$$

[1] https://github.com/MyoHub/myosuite/blob/main/docs/source/tutorials/6_Inverse_Dynamics.ipynb

Algorithm	Parameter	Task	
		Stand	Walk
SAC	Learning rate	linear schedule(0.001)	
	Batch size	256	
	Buffer size	1e6	
	Warmup steps	100	
	Discount factor	0.98	
	Soft update coeff.	2	
	Train frequency (steps)	1	
	Gradient steps	4	
	Target update interval	1	
	Environment number	112	
	Entropy coeff.	auto	
	Target entropy	auto	
	Policy hiddens	[512, 300]	
	Q hiddens	[512, 300]	
	Activation	ReLU	
	Training steps	1e7	
DynSyn	Control Amplitude	5	
	Trajectory steps	5e5	
	Number of groups	100	
	aD	3e7	
	kD	5e-9	

Table 1: Parameters of SAC and DynSyn

where f_{max} is the maximum isometric muscle force, and a, l, and v represent the activation, normalized length, and normalized velocity of the muscle, respectively. The term $F_p(l)$ accounts for the passive force-length relationship, and the terms $F_l(l)$ and $F_v(v)$ are the force-length and force-velocity functions, which have been fitted using data from biomechanical experiments (Millard et al., 2013).

We use the following 37 major joint positions that determine the whole-body posture: hip (6) knee (2), ankle (2), subtalar (4), spinal (9), shoulder (6), elbow (2), and wrist (6).

B BASELINES

We compare our algorithm with the reinforcement learning algorithms DynSyn. DynSyn adopt SAC as the basic algorithm and use the DRL framework Stable baselines3. We set control frequency to 10 simulation steps, which can significantly increase the sample efficiency of the reinforcement learning algorithm. All the parameters are reported in the original papers, and we use the same parameters for models with similar complexity. Algorithm hyperparameters are summarized in Table 1.

The output range of the reinforcement learning policy is typically $[-1, 1]$, and it is then normalized to $[0, 1]$ in order to control the musculoskeletal system. We use the following equation to normalize the action of the policy, which is widely used in MyoSuite environments.

$$a = \frac{1}{1 + e^{-5(a-0.5)}}$$

The reward design is as follows:

$$\text{reward} = \text{reward}_{\text{health}} - \text{cost}_{\text{tasks}}$$

where $reward_{\text{health}}$ is the healthy reward given in each step, We subtract $\text{cost}_{\text{tasks}}$ and add it to $reward_{\text{health}}$ to ensure that the reward remains positive. We find that the original cost weight in the cost function is sufficient for the reinforcement learning algorithm to learn effectively, so we adopt the same weight as used in the cost function.

C TASK SETTINGS

The common objective terms are defined as follows:

Height. This term encourages maintaining a specific height between the head and feet. It only penalize when the head is too low.

$$cost_{height} = |\min(H_{head} - H_{feet} - H_{target}, 0)|$$

where H_{head} is the head height, H_{feet} is the average height of the four feet, and H_{target} is the target height (different for each task).

Upright. This term encourages the character to maintain an upright posture.

$$cost_{upright} = \left|(1 - \hat{k}_{up} \cdot \hat{k}_{pelvis}) + (1 - \hat{k}_{up} \cdot \hat{k}_{head}) + 0.1(1 - \hat{k}_{up} \cdot \hat{k}_{lfoot}) + 0.1(1 - \hat{k}_{up} \cdot \hat{k}_{rfoot})\right|$$

where $\hat{k}_{up}$ is the up direction vector, and $\hat{k}_{head}$, $\hat{k}_{torso}$, $\hat{k}_{pelvis}$, $\hat{k}_{lfoot}$, $\hat{k}_{rfoot}$ are the up vectors for the head, torso, pelvis, left foot, and right foot respectively.

Balance. This term encourages keeping the center of mass above the support polygon formed by the feet.

$$cost_{balance} = |\mathbf{COM}_{xy} - \mathbf{F}_{avg}|$$

where $\mathbf{COM}_{xy}$ is the horizontal position of the center of mass, and $\mathbf{F}_{avg}$ is the average horizontal position of the feet.

Forward velocity. This term encourages maintaining a specific forward velocity.

$$cost_{forwardvelocity} = \left|\mathbf{v}_{com} \cdot \hat{k}_{forward} - v_{target}\right|$$

where $\mathbf{v}_{com}$ is the center of mass velocity, $\hat{k}_{forward}$ is the forward direction vector, and v_{target} is the target velocity.

Forward angle. This term discourages sideways motion.

$$cost_{forwardangle} = \left\|\mathbf{v}_{com} - (\mathbf{v}_{com} \cdot \hat{k}_{forward})\hat{k}_{forward}\right\|_2$$

Pelvis forward. This term encourages the character to face forward.

$$cost_{forward} = \left|(1 - \hat{k}_{forward} \cdot \hat{k}_{pelvis})\right|$$

where $\hat{k}_{pelvis}$ is the forward direction of the pelvis.

Joint velocity. This term penalizes excessive joint velocities.

$$cost_{jointvelocity} = \|\mathbf{q}_{vel}\|_2$$

where $\mathbf{q}_{vel}$ is the vector of joint velocities.

Joint position. This term penalizes extreme joint positions.

$$cost_{jointposition} = \|\mathbf{q}_{pos}\|_2$$

where $\mathbf{q}_{pos}$ is the vector of joint positions.

Feet cross. This term discourages crossing of the feet and maintains proper leg alignment.

$$cost_{feetcross} = \left|\min(0, \hat{k}_{hip} \cdot \hat{k}_{feet} - 0.15) + \min(0, \hat{k}_{hip} \cdot \hat{k}_{toe} - 0.15) + \min(0, \hat{k}_{hip} \cdot \hat{k}_{knee} - 0.15)\right|$$

where $\hat{k}_{hip}$, $\hat{k}_{feet}$, $\hat{k}_{toe}$, $\hat{k}_{knee}$ are the direction vector between hip joints, feet centers, toes and knee joints.

We list the cost function setting of tasks in Table 2. For the soccer tasks, we set the cost terms are position errors berween motion capture points and current body part, with weight shown in Figrue 7.

Cost Function Term	Tasks				
	Stand	Walk	Rough	Slope	Stair
Height	100				
Upright	100				
Balance	100				
Forward velocity	10				50
Forward angle	10				20
Pelvis forward	100				
Joint velocity	0.01	/	/	/	/
Joint position	1	5	2		
Feet cross	/	50			

Table 2: Weights of Cost functions

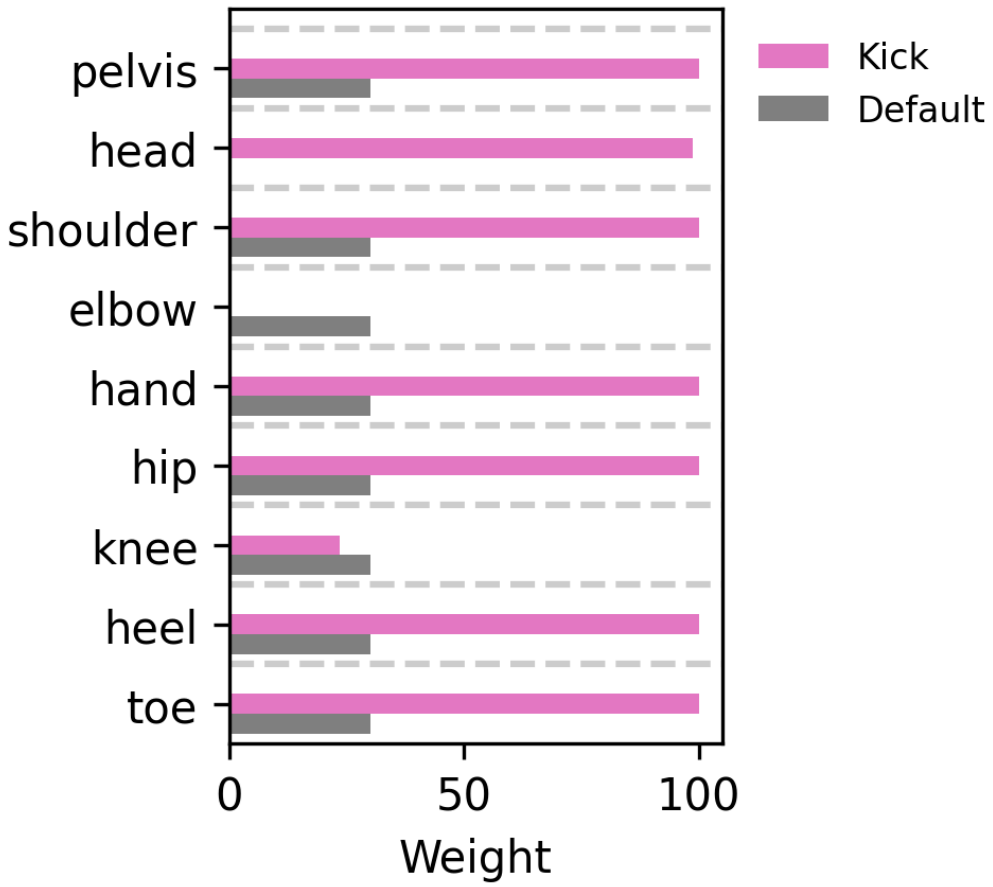

Figure 7: Cost initial and optimized weight of the Soccer task.